

# The variability of hydrogen-bonded supramolecular assemblies in crystalline picrates prepared from ferrocenyl-substituted $\beta$ -aminoalcohols

Petr Štěpnička<sup>a,\*</sup>, Martin Zábbranský<sup>a</sup>, Martin Lamač<sup>a</sup>, Ivana Císařová<sup>a</sup>, Petr Němec<sup>b</sup>

<sup>a</sup> Charles University in Prague, Faculty of Science, Department of Inorganic Chemistry, Hlavova 2030, 128 40 Prague, Czech Republic

<sup>b</sup> Charles University in Prague, Faculty of Mathematics and Physics, Department of Chemical Physics and Optics, Ke Karlovu 3, 121 16 Prague, Czech Republic

Received 21 December 2007; received in revised form 22 January 2008; accepted 23 January 2008

Available online 2 February 2008

## Abstract

Ferrocene-based  $\beta$ -aminoalcohols  $\text{FcCH}_2\text{NHCR}_2\text{CH}_2\text{OH}$  ( $\text{R} = \text{H}$ , **1a**;  $\text{R} = \text{Me}$ , **1b**) and (*S*)- $\text{FcCH}_2\text{NHCH}(\text{CHMe}_2)\text{CH}_2\text{OH}$  (**1c**; Fc = ferrocenyl) react with 2,4,6-trinitrophenol (Hpic) under proton transfer to afford the corresponding ammonium picrates **2a–c**. In the crystal, these picrates associate predominantly via  $\text{N–H}\cdots\text{O}$  and  $\text{O–H}\cdots\text{O}$  bifurcated hydrogen bonds between the  $\text{NH}_2^+$  and OH groups in the aminoalcohol chain as the donors and the phenoxide and  $\text{NO}_2$  oxygen atoms of the picrate anion as the acceptors. Compounds **2a** and **2b** form closed dimeric assemblies  $[\text{InH}]_2[\text{pic}]_2$  ( $\text{n} = \text{a, b}$ ) around the crystallographic inversion centres. By contrast, their chiral analogue **2c** gives rise to monomeric units  $[\text{IcH}][\text{pic}]$  (albeit through similar interactions), that further aggregate into infinite linear chains via  $\text{N–H}\cdots\text{O}$  hydrogen bonds. The formed assemblies are interconnected by the soft  $\text{C–H}\cdots\text{O}$  hydrogen bonds and via  $\pi\cdots\pi$  stacking interactions of the picrate ions.

© 2008 Elsevier B.V. All rights reserved.

**Keywords:** Ferrocene; Aminoalcohols; Picrates; Chirality; Crystal structure

## 1. Introduction

The design and preparation of ordered metal–organic solids from organometallic precursors represent an attractive approach towards new functional materials [1]. Despite the recent effort, the synthesis of defined crystalline materials is still far from rational and typically relies on spontaneous self-assembly of molecular building blocks via non-covalent interactions. Hence, the synthesis of defined building blocks and studies into their structural properties are desirable in order to provide a sound base for their subsequent use in the preparation of crystalline materials.

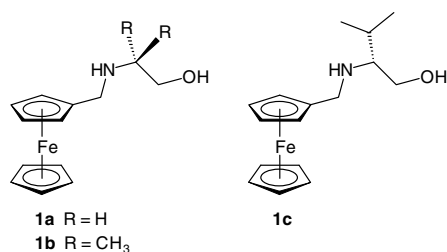
Polar ferrocene derivatives appear to be particularly suitable precursors to defined crystalline materials as they

combine high chemical stability with unique physicochemical properties of the ferrocene framework [2]. However, the number of ferrocene compounds that have been utilised in creating supramolecular architectures remains rather low and, above all, limited to few ligand classes. The typical examples include ferrocene-based carboxylic acids [3], alcohols [4] and heterocycles [5]. This initiated our interest in the preparation of polar ferrocene derivatives that are capable of forming *multiple* hydrogen bonds [6]. We chose these compounds mainly because of the fairly high stability and better predictability of the hydrogen-bonded assemblies as compared to systems featuring the relatively weaker  $\text{C–H}\cdots\text{X}$  ( $\text{X} = \text{heteroatom}$  or  $\pi$ -system) and  $\pi\cdots\pi$  interactions [7].

In our previous work, we had focused on ferrocenyl-methanol derivatives substituted with phosphorus groups at the ferrocene unit [8] and, later, turned to compounds with  $\beta$ -hydroxyamine pendant chains. So far, we have

\* Corresponding author. Fax: +420 221 951 253.

E-mail address: stepnic@natur.cuni.cz (P. Štěpnička).



Scheme 1.

prepared and structurally characterised a series of ferrocene carboxamides bearing 2-hydroxyethyl groups at the amide nitrogens [9], and reported the crystal structures of ferrocene  $\beta$ -aminoalcohol **1b** (Scheme 1) and its ammonium salts [10].

Because the latter study revealed a pronounced effect of the anion on the crystal assembly, we decided to study also the influence of the substituents at the aminoalcohol chain in a series of ammonium salts featuring the same anion. As the anion source we chose 2,4,6-trinitrophenol (picric acid) which is known to form well-defined crystalline salts with amines and, simultaneously, possesses a number of potential hydrogen-bond acceptors. In this contribution we describe the preparation and crystal structures of picrates from aminoalcohols **1a–c** (Scheme 1). In addition, we present the results of UV–Vis spectroscopic and second harmonic generation (SHG) measurements for the chiral picrate obtained from **1c**.

## 2. Results and discussion

### 2.1. Syntheses and characterisation

Aminoalcohols **1a–c** (Scheme 1), readily available from ferrocenecarboxaldehyde and the respective  $\beta$ -aminoalcohols [10,11], react smoothly with 2,4,6-trinitrophenol (Hpic) under proton transfer to afford the respective ammonium picrates **2a–c**. Upon slow addition of hexane, the picrates separate directly from the reaction solution as air-stable, burgundy red crystalline solids.

Because of the known sensitivity of picrates to heating, impact or friction, we have firstly studied the thermal stability of the compounds to avoid possible problems. Fortunately, compounds **2a–c** are thermally rather stable, decomposing above ca. 150 °C. When heated in an open test tube, they vigorously decompose leaving dark voluminous, soot-like residua. On the other hand, they can be pulverised in a mortar without any appreciable decomposition.

As the mixing of the yellow (Hpic) and orange (aminoalcohols) educts in ethyl acetate affords yellow solutions from which deep red crystalline products separate, we have investigated the spectral properties of the **1c**-picric acid model system in the UV–Vis region. Fig. 1 indicates that the spectra of picric acid and compound **2c** are practically identical, showing a band at 354 nm and a shoulder at around 400 nm [12]. By contrast, the spectrum of solid **2c**

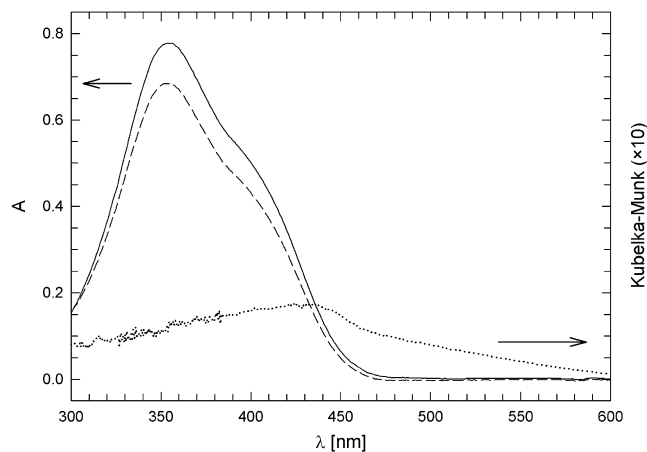


Fig. 1. UV–Vis spectra of **2c** (solid line) and 2,4,6-trinitrophenol (dashed line) in methanol solutions ( $c = 5 \times 10^{-5}$  M, optical path 10 mm) and the spectrum of solid **2c** (dotted line; diffuse reflectance mode, a powdered sample was diluted with BaSO<sub>4</sub>).

displays a broad maximum shifted by about 80 nm to lower energies. This shift probably reflects the formation of  $\pi \cdots \pi$  interacting assemblies in the solid state (see below) that either open new pathways for optical electron transfer processes or at least influence the distribution of the energy levels.

Since many ferrocene derivatives [2c,13] including supramolecularly assembled ones [13e] as well as picric acid and its salts or adducts [14] exert non-linear optical properties, we have tested the chiral picrate **2c** for second-harmonic generation (SHG) efficiency. Indeed, the compound showed some frequency doubling when irradiated at 800 nm. However, a powdered sample (size fraction 75–125  $\mu\text{m}$ ) of **2c** was found to have SHG efficiency of only 1.1% that of urea.

### 2.2. Molecular structures of **2a–c**

Views of the molecular structures of **2a–c** are shown in Figs. 2–4, respectively, and the selected geometric parameters are summarised in Table 1 and in Fig. 5. In all three cases, the geometry of the ferrocene units is regular, showing nearly identical Fe–Cg (see Table 1 for definitions) and negligible tilts. The interatomic distances and angles within the protonated aminoalcohol pendant chains are similar and also compare favourably with the data reported for unprotonated **1b** and its bromide and dihydrogenphosphate salts [10]. The most notable difference is seen in the conformation of the aminoalcohol chain. The torsion angles at the C11–N1 and C12–C13 bonds change by only ca. 10° in the whole series, whilst the torsion angle C11–N1–C12–C13 varies broadly from ca. 76° for **2b** to ca. 180° for **2a**. This is, however, the likely consequence of the crystal packing effects: Whereas the torsion around the C12–C13 bond controls the orientation of the polar groups, which is kept near to synclinal, the rotation along the C11–N1 bond may facilitate the accommodation of the

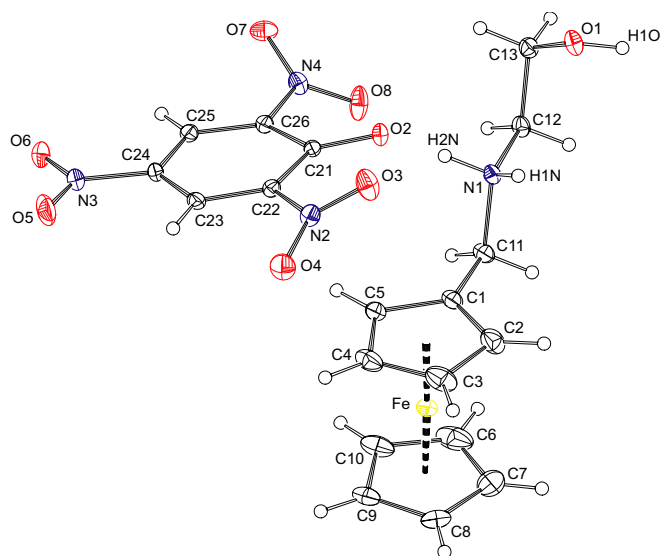


Fig. 2. The molecular structure of **2a**. Displacement ellipsoids are drawn with 30% probability.

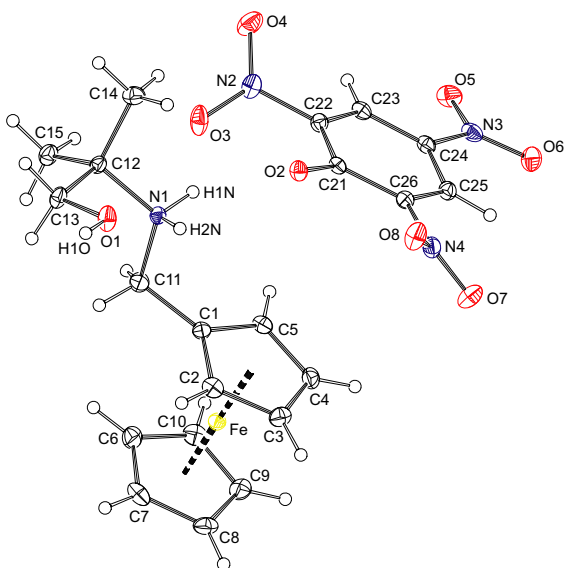


Fig. 3. The molecular structure of **2b**. Displacement ellipsoids are drawn with 30% probability.

bulky ferrocene moiety in the crystal (see the discussion of the crystal packing).

The structures of the picrate counter ions in **2a–c** are similar (Fig. 5); the only statistically significant difference in the interatomic distances is found among the C22–C23 bond lengths. The picrate moiety displays partial quinoid character where the C–C bonds adjoining the phenoxide carbon atom C21 are markedly longer than the remaining inter-ring C–C bonds. The C21–O2 distance corresponds well with the distances typically encountered in the crystal structures of simple organic picrates, including the  $\beta$ -aminoalcohol-based ones possessing 2-hydroxyethanaminium (1.260 Å) [15], (2-hydroxymethyl)trimethylammonium

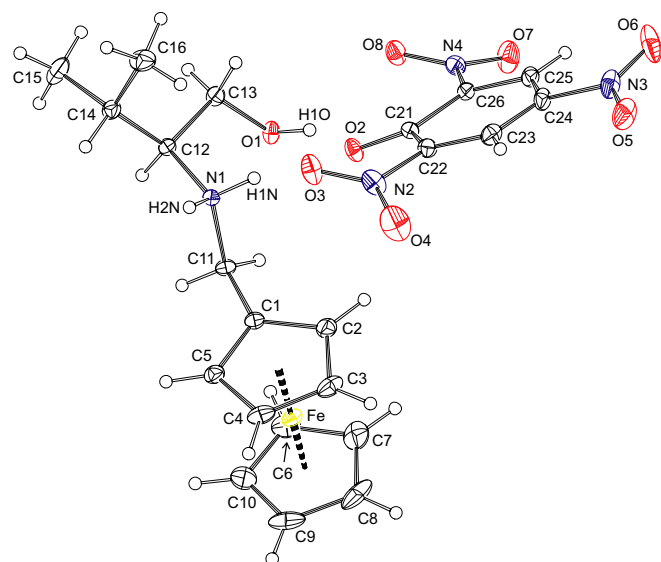


Fig. 4. The molecular structure of **2c**. Displacement ellipsoids are drawn with 30% probability.

Table 1

Selected distances and angles for **2a**, **2b**, and **2c** (in Å and °)<sup>a,b</sup>

Parameter	<b>2a</b>	<b>2b</b>	<b>2c</b>
Fe–Cg1	1.6445(8)	1.6419(8)	1.6420(9)
Fe–Cg2	1.650(1)	1.6512(9)	1.646(1)
$\angle$ Cp1,Cp2	1.7(1)	1.1(1)	0.3(1)
N1–C11	1.503(2)	1.511(2)	1.518(2)
N1–C12	1.487(2)	1.525(2)	1.517(2)
O1–C13	1.413(2)	1.419(2)	1.430(2)
C1–C11–N1–C12	177.9(1)	168.3(2)	167.3(1)
C11–N1–C12–C13	–179.9(1)	75.7(2)	–95.7(2)
N1–C12–C13–O1	55.9(2)	49.0(2)	48.8(2)
Cp1···Pic	4.7701(9)	5.127(1)	ca. 6.08
$\angle$ Cp1,Pic	11.64(9)	14.11(9)	31.4(1)

<sup>a</sup> The ring planes are defined as follows: Cp1 = C(1–5), Cp2 = C(6–10), Pic = C(21–26). Cg1, Cg2 and CgP denote their respective ring centroids.

<sup>b</sup> Interatomic distances for the picrate ions are summarised in Fig. 5.

(1.243(2) Å) [16], and 4,4-bis(2-hydroxyethyl)-1-oxa-4-azoniacyclohexane (1.234(7) Å) [17] as the cations.

The planes of the nitro substituents show different rotations from the plane of their parent aromatic ring. The maximum dihedral angle is ca. 45° for the {N2O3O4} group in **2a** whereas the lowest rotation by ca. 5° is exerted by the {N3O5O6} groups in **2a** and **2c**. The rotation of the nitro groups is probably brought about by steric interference between the phenoxide oxygen and its adjacent nitro groups and also by crystal packing forces, e.g., hydrogen bonding interactions, the formation of which may well compensate a destabilisation resulting from a reduced conjugation of the  $\pi$ -systems.

Although the picrate aromatic ring does not deviate much from coplanarity with the ferrocene cyclopentadienyl Cp1 in both **2a** and **2b**, the rings are rather distant to allow for an efficient  $\pi$ ··· $\pi$  interaction. In the case of compound **2c**, the distance and rotation of the ring planes are even less favourable (Table 1).

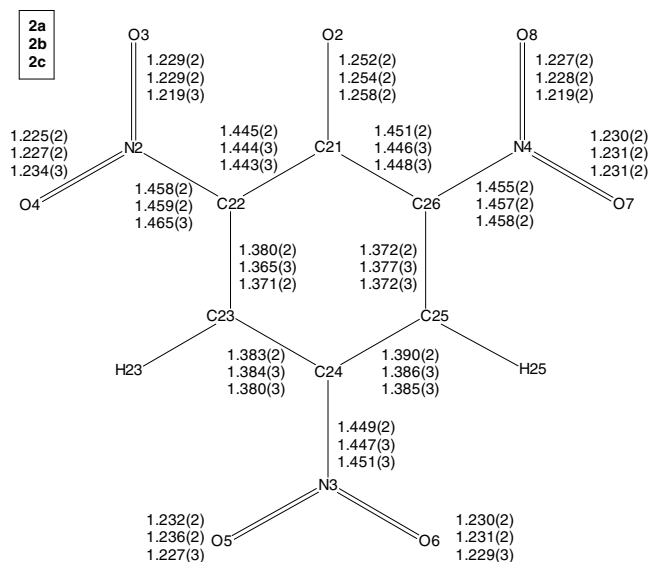


Fig. 5. Summary of the bond lengths for the picrate anions in **2a–c** (in Å).

### 2.3. Description of the crystal packing

Views of the crystal packing of **2a** are shown in Fig. 6 and the relevant geometric data are presented in Table 2. The basic repeating unit in the crystal of **2a** is constituted by two ion-pairs [1aH][pic] that assemble into centrosymmetric dimers (Fig. 6a). The cation–anion secondary bonding in the resulting four-ion aggregate is accomplished exclusively via a pair of three-centre hydrogen bonds from the NH and OH protons at the aminoalcohol chain to the

Table 2  
Summary of hydrogen bond parameters for **2a–c** (in Å and °)<sup>a</sup>

D–H···A	D···A	Angle at H
<b>Compound 2a</b>		
N1–H1N···O1 <sup>i</sup>	2.748(2)	146
N1–H1N···O1	2.869(2)	128
N1–H2N···O2	2.778(2)	148
O1–H1O···O2 <sup>i</sup>	2.680(2)	131
O1–H1O···O3 <sup>i</sup>	3.140(2)	150
C12–H12A···O8	2.970(2)	105
C12–H12B···O6 <sup>ii</sup>	3.234(2)	137
<b>Compound 2b</b>		
N1–H1N···O2	2.849(2)	144
N1–H1N···O3	3.025(2)	137
N1–H2N···O1	2.697(2)	112
N1–H2N···O1 <sup>iii</sup>	2.892(2)	143
O1–H1O···O2 <sup>iii</sup>	2.670(2)	154
O1–H1O···O8 <sup>iii</sup>	3.022(2)	128
C4–H4···O4 <sup>iv</sup>	3.430(3)	156
C13–H13A···O8 <sup>iii</sup>	2.977(3)	111
C13–H13A···O5 <sup>v</sup>	3.255(2)	143
C14–H14A···O3	3.337(3)	136
C15–H15C···O3	3.285(3)	139
<b>Compound 2c</b>		
N1–H1N···O2	2.852(2)	142
N1–H1N···O3	3.127(2)	139
N1–H2N···O1 <sup>vi</sup>	2.777(2)	171
O1–H1O···O2	2.646(2)	150
O1–H1O···O8	2.816(2)	125
C8–H8···O7 <sup>vii</sup>	3.381(3)	151
C11–H11···O6 <sup>viii</sup>	3.438(3)	149

<sup>a</sup> D = donor, A = acceptor. Symmetry codes: (i)  $-x, -y, 1 - z$ ; (ii)  $x, y, -1 + z$ ; (iii)  $-1 - x, 1 - y, -z$ ; (iv)  $-x, 1/2 + y, 1/2 - z$ ; (v)  $-1 + x, y, z$ ; (vi)  $2 - x, 1/2 + y, 2 - z$ ; (vii)  $2 - x, 1/2 + y, 1 - z$ ; (viii)  $1 + x, y, 1 + z$ .

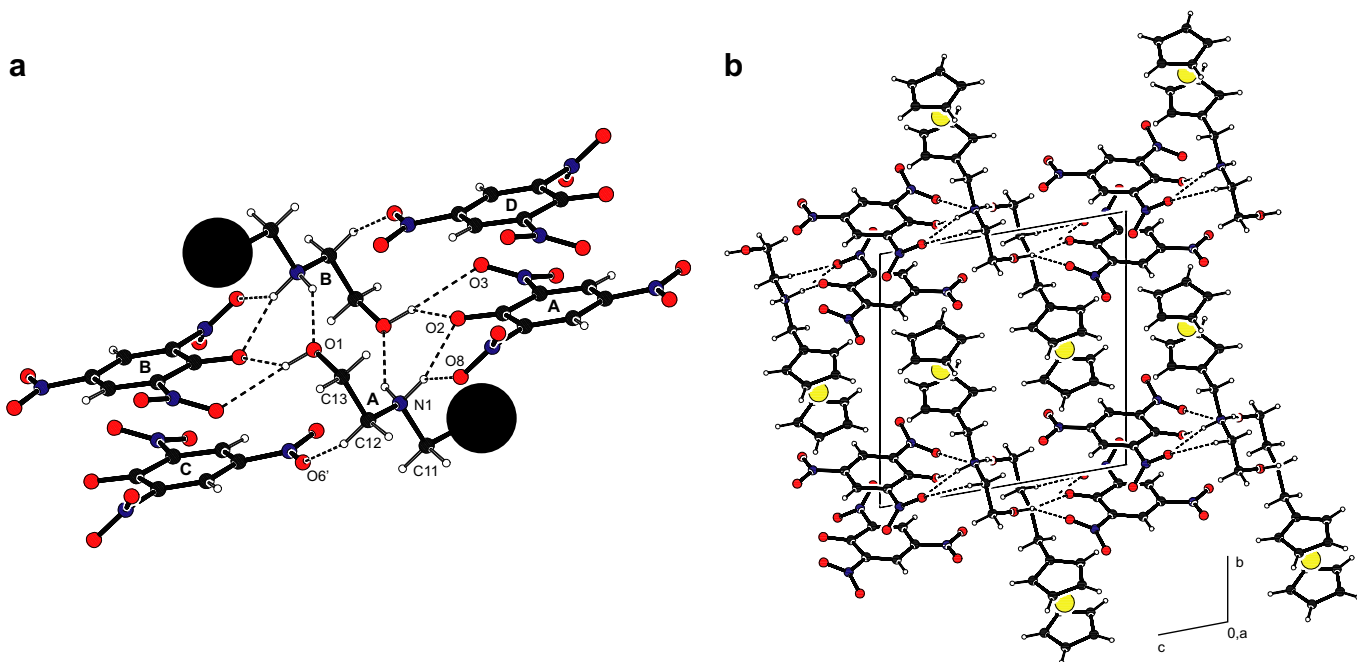


Fig. 6. (a) Principal intermolecular interactions in the structure of **2a**. To avoid overlaps, the bulky ferrocenyl groups were replaced with filled black circles. The hydrogen bonds are shown as dashed lines. Symmetry operations: A ( $x, y, z$ ); B ( $-x, -y, 1 - z$ ); C ( $x, y, -1 + z$ ); D ( $-x, -y, 2 - z$ ). (b) View of the unit cell of **2a** along the crystallographic  $a$ -axis.

picrate oxygen atoms ( $O^-$  and  $NO_2$ ). The aminoalcohol chains are interconnected through the two-centre  $N1-H2N \cdots O1$  hydrogen bonds (Table 2).

The formed assembly is further linked to two adjacent picrate ions generated by translation along the  $c$ -axis ( $A \rightarrow C$  and  $B \rightarrow D$  in Fig. 6a). The adjacent picrate ions interact via cooperative  $\pi \cdots \pi$  stacking interactions of their per-symmetry parallel benzene rings at the centroid-centroid distance  $pic \cdots pic'$  of 3.4076(8) Å (the prime-labelled plane is generated by the inversion operation  $(-x, -y, 2-z)$ ; cf. interplanar distance = 3.29 Å, ring slippage = 0.90 Å; pairs  $A \cdots D$  and  $B \cdots C$  in Fig. 6a) and by thus enforced  $C-H \cdots O$  contacts between the picrate oxygen atoms  $O6$  and  $O8$  and hydrogens at  $C12$  (Table 2). When combined, these interactions result into the formation of infinite chains along the crystallographic  $c$ -axis. These chains are located in the  $ac$  plane at  $b = 0$  and 1, forming polar layers that are separated by non-polar domains built up from the alternating ferrocene moieties (Fig. 6b).

The crystal assembly of **2b** (Fig. 7, Table 2) resembles in many regards the packing of its non-methylated analogue **2a**. The observed differences seem to reflect increased steric bulk of the polar hydroxyamine chain, which also results in conformational changes. On going from **2a** to **2b**, the  $N1-C12-C13-O1$  angle becomes by ca.  $7^\circ$  smaller while the  $C11-N1-C12-C13$  angle drops from a value typical for an antiperiplanar arrangement to synclinal (see Table 1). Consequently, both methyl groups are directed away from the OH and  $NH_2$  groups involved in hydrogen bonding interactions.

Similarly to **2a**, the key feature in the crystal assembly of **2b** is a centrosymmetric dimer involving two  $[1bH][pic]$  ion-pairs, where the cations and anions interact via bifurcated  $N1-H1N \cdots O(pic)$  and  $O1-H1O \cdots O(pic)$  hydrogen bonds whereas the hydroxyammonium chains are connected by

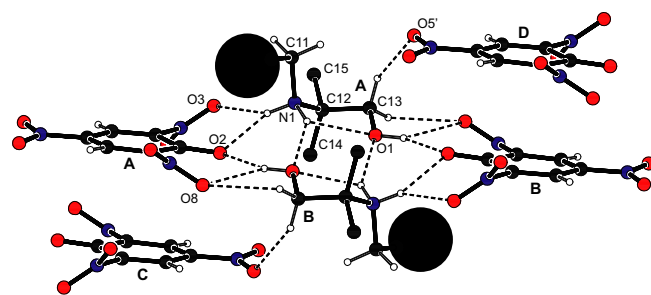


Fig. 7. Intermolecular interactions in the structure of **2b**. The ferrocenyl groups were replaced with black circles and the hydrogen bonds are indicated with dashed lines. Symmetry operations: A ( $x, y, z$ ); B ( $-1-x, 1-y, -z$ ); C ( $-x, 1-y, -z$ ); D ( $-1+x, y, z$ ).

the  $N1-H2N \cdots O1$  hydrogen bonds. The changed conformation of the aminoalcohol chain together with re-orientation of the subunits allows for an increase in the number of hydrogen bonding interactions. When compared with **2a**, the structure of **2b** features an additional  $C-H \cdots O(pic)$  contact per one molecule and, more importantly, an intramolecular  $N1-H2N \cdots O1$  hydrogen bond that apparently stabilises the conformation of the hydroxyammonium chain.

As in the case of **2a**, the dimers of **2b** aggregate with picrate ions from the neighbouring units via cooperative  $C-H \cdots O(pic)$  contacts and offset  $\pi \cdots \pi$  stacking interactions of the parallel aromatic rings (Fig. 7;  $A \cdots C$  and  $B \cdots D$ : centroid-centroid distance = 3.474(1) Å, interplanar separation = 3.39 Å, offset of the planes = 0.75 Å).

The crystal assembly of picrate **2c** markedly differs from its achiral counterparts mainly because the chiral compound cannot form closed centrosymmetric assemblies (Fig. 8a). Thus, instead of interacting with a pair of the cations (as in **2a** and **2b**), each picrate ion in **2c** binds to a single aminoalcohol moiety by two three-centre hydrogen

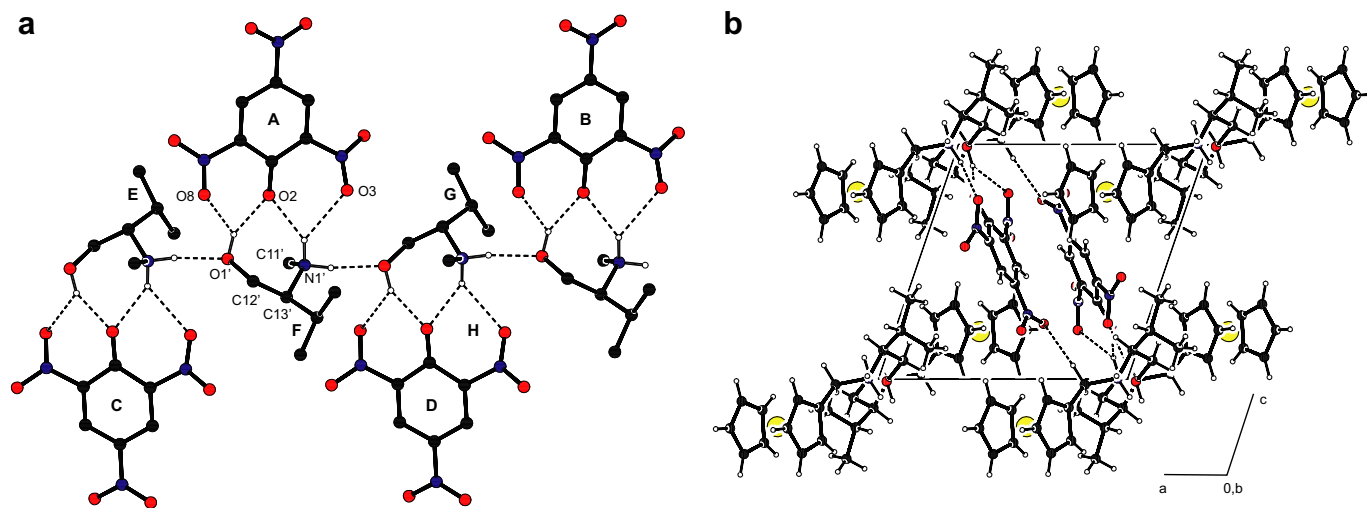


Fig. 8. (a) View of the hydrogen-bonded chains in the structure of **2c**. The ferrocenyl moieties are omitted for clarity. (b) A projection of the unit cell onto the  $ac$  plane. The hydrogen bonds are indicated with dashed lines. Symmetry operations: A ( $x, y, z$ ); B ( $x, 1+y, z$ ); C ( $2-x, -1/2+y, 2-z$ ); D ( $2-x, 1/2+y, 2-z$ ); E ( $1-x, -1/2+y, 2-z$ ); F ( $1+x, y, z$ ); G ( $1-x, 1/2+y, 2-z$ ); H ( $1+x, 1+y, z$ ).

bonds involving the phenoxide O2 and one oxygen atom from both adjacent NO<sub>2</sub> groups as the acceptors, and the OH and NH protons as the donors. The formed ion pairs associate linearly into infinite angular chains along the crystallographic 2<sub>1</sub> screw axes by means of hydrogen bond between the second NH proton and the hydroxyl oxygen from an adjacent molecule (see Table 2 for hydrogen bond parameters). Contrary to the previous cases, the structure lacks any significant  $\pi \cdots \pi$  interactions, the cross-linking of the hydrogen-bonded chains being achieved through the relatively softer C–H $\cdots$ O interactions (Fig. 8b).

### 3. Conclusions

In summary, the reaction of ferrocene aminoalcohols **1a–c** with picric acid affords well defined and reasonably stable crystalline picrates **2a–c**. The chief force towards intermolecular association of these salts are N–H $\cdots$ O(pic) and O–H $\cdots$ O(pic) hydrogen bonds that are supported by C–H $\cdots$ O contacts and by offset  $\pi \cdots \pi$  stacking interactions of the parallel benzene rings. Whereas the former interactions are typically responsible for the formation of closed centrosymmetric assemblies or at least the basic repeating unit such in **2c**, the latter represent the means for a further supramolecular aggregation. The formed structures are rather compact, showing similar space filling efficiencies (70.6% for **2b**, 70.5% for **2b**, and 68.7 for **2c**). The density of the picrates parallels the trend in space filling, being lowest for the chiral representative, whose structure lacks the cyclic aggregates.

A closer look at the structures reveals that the phenoxide oxygen atom O2 always points towards the twisted aminoalcohol chain and forms the shortest hydrogen bonds with the NH and OH protons. This indicates that electrostatic interactions play significant role in stabilisation of the supramolecular arrays (e.g., via charge-support to the hydrogen bonding interactions). Furthermore, it is evident that the excess of the potential hydrogen bond donors in the structures of **2a–c** leads to preferential formation of three-centre hydrogen bonds with bifurcated donors that in turn give rise to structure-stabilising cyclic (chelate) subunits.

### 4. Experimental

#### 4.1. Methods

NMR spectra were measured on a Varian UNITY Inova 400 spectrometer at 298 K. Chemical shifts ( $\delta$ /ppm) are given relative to internal tetramethylsilane. IR spectra were recorded on an FT-IR Nicolet Magna 760 instrument in the range of 400–4000 cm<sup>-1</sup>. UV–Vis spectra were recorded with Unicam UV300 (solution) and on a Perkin–Elmer Lambda 35 spectrometers (solid state). The samples were dissolved in methanol or powdered and diluted with barium sulphate (Merck, white standard). Optical rotations

were measured with an automatic polarimeter Autopol III (Rudolph Research) at room temperature. Positive ion electron impact (EI+) mass spectra including the high resolution (HR) measurements were performed with a ZAB EQ spectrometer (VG Analytical). Melting points were determined on a Kofler block.

The measurements of SHG efficiency were performed using the Kurtz powder method [18] at 800 nm with pulse Ti-sapphire laser (Tsunami, Spectra Physics; 90 fs pulse width, 82 MHz repetition rate). For quantitative determination of the SHG efficiency, the intensity of the back-scattered laser light at 400 nm was measured by a grating spectrograph with a diode array (InstaSpec II, Oriel) and its intensity was compared with that of a urea standard. To minimise the influence of preferential orientation, the experiments were performed on powdered samples (75–125  $\mu$ m particle size) loaded into a 5 mm glass cell with the aid of a vibrator, and the measurements were repeated on different areas of the sample.

**Safety Note. CAUTION!** Although we have not encountered any problems it should be noted that picrates are potentially explosive and should be handled with care.

#### 4.2. Syntheses

The aminoalcohols have been prepared by reduction of the (non-isolated) intermediate imines resulting from condensation of ferrocenecarboxaldehyde with the respective aminoalcohol. The preparation of **1a** [11] and **1b** [10] was reported elsewhere; compound **1c** was synthesised as follows.

##### 4.2.1. Preparation of (*S*)-2-[(ferrocenylmethyl)amino]-3-methyl-butan-1-ol (**1c**)

Ferrocenecarboxaldehyde (428 mg, 2.0 mmol) and (*S*)-valinol (217 mg, 2.1 mmol) were dissolved in dry chloroform (20 mL; dried over K<sub>2</sub>CO<sub>3</sub>) and the resulting solution was heated at reflux under argon for 90 min. Then, the solution was cooled to room temperature, the solvent was removed under vacuum and the red–brown residue immediately re-dissolved in dry methanol (20 mL; distilled from a MeONa solution). The methanolic solution was cooled in an ice bath and treated slowly with solid NaBH<sub>4</sub> (378 mg, 10 mmol over 30 min). After the addition was complete, the mixture was stirred at 0 °C for 1 h and at room temperature for 90 min. Then, it was quenched by addition of 10% aqueous NaOH (20 mL) and extracted with dichloromethane (2  $\times$  20 mL). The combined organic layer was washed with brine (2  $\times$  20 mL), dried over magnesium sulphate, and evaporated, leaving the crude product as a yellow–brown solid. Subsequent purification by column chromatography (silica gel, dichloromethane–methanol 10:1) led to the development of two bands: the first (minor) one containing mostly ferrocenylmethanol, followed by the major band of the aminoalcohol. Careful evaporation of the second fraction afforded pure **1c** as an amber oil, which slowly solidifies to a brown solid. Yield: 457 mg (76%).

$[\alpha_D]^{23\text{ }^\circ\text{C}} + 20.4^\circ$  ( $c = 1.0$ ,  $\text{CHCl}_3$ ).  $^1\text{H}$  NMR (400 MHz,  $\text{CDCl}_3$ ):  $\delta$  0.91, 0.97 (2  $\times$  d,  $^3J_{\text{HH}} = 6.8$  Hz, 3H,  $\text{CH}_2\text{Me}$ ); 1.84 (octet,  $^3J_{\text{HH}} = 6.8$  Hz, 1 H,  $\text{CHMe}_2$ ), 2.47 (dt,  $^3J_{\text{HH}} = 4.2$ , 6.7 Hz, 1H,  $\text{CHNH}$ ), 2.71 (br s, 2H,  $\text{NH}$  a  $\text{OH}$ ), 3.38 (dd,  $^2J_{\text{HH}} = 10.7$ ,  $^3J_{\text{HH}} = 6.9$  Hz, 1H,  $\text{CH}_2\text{OH}$ ), 3.52 and 3.56 (2  $\times$  d,  $^2J_{\text{H}} = 12.9$  Hz, 1H, AB system of  $\text{FcCH}_2$ ); 3.63 (dd,  $^2J_{\text{HH}} = 10.7$ ,  $^3J_{\text{HH}} = 4.2$  Hz, 1H,  $\text{CH}_2\text{OH}$ ), 4.12 (m, 2H,  $\text{C}_5\text{H}_4$ ), 4.13 (s, 5H,  $\text{C}_5\text{H}_5$ ), 4.20 (virtual t, 2H,  $\text{C}_5\text{H}_4$ ).  $^{13}\text{C}\{^1\text{H}\}$  NMR (100 MHz,  $\text{CDCl}_3$ ):  $\delta$  18.52, 19.65 ( $\text{CHMe}_2$ ); 28.86 ( $\text{CHMe}_2$ ), 46.34 ( $\text{FcCH}_2$ ), 60.28 ( $\text{CH}_2\text{OH}$ ), 63.96 ( $\text{CHNH}$ ), 67.80, 67.92, 68.09, 68.25 (CH of  $\text{C}_5\text{H}_4$ ); 68.40 ( $\text{C}_5\text{H}_5$ ), 86.51 ( $C_{\text{ipso}}$  of  $\text{C}_5\text{H}_4$ ). IR (neat):  $\nu/\text{cm}^{-1}$  3311 s, 3277 s, 3092 br, 2957 vs, 2932 m, 2870 vs, 2825 vs, 2118 m, ca. 1550–1790 br m, 1466 s, 1438 s, 1385 s, 1361 m, 1332 w, 1308 w, 1234 m, 1196 m, 1104 vs, 1083 m, 1050 s, 1040 s, 998 vs, 976 s, 923 m, 914 m, 907 m, 857 s, 829 s, 816 vs, 809 vs, 752 w, 693 br w, 562 w, 537 w, 490 vs, 478 vs, 427 m. EI MS:  $m/z$  (relative abundance) 302 (7), 301 (33,  $M^+$ ), 299 (2), 215 (1), 200 (16), 199 (100,  $[\text{FcCH}_2]^+$ ), 197 (6), 186 (2,  $\text{FcH}^+$ ), 165 (3), 147 (4), 135 (4), 121 (30,  $[\text{C}_5\text{H}_5\text{Fe}]^+$ ), 56 (13,  $\text{Fe}^+$ ). Anal. Calc. for  $\text{C}_{16}\text{H}_{23}\text{FeNO}$  (301.2): C, 63.80; H, 7.70; N, 4.65. Found: C, 63.26; H, 7.84; N, 4.42%.

#### 4.2.2. General procedure for the preparation of the picrates

Picric acid (23 mg, 0.10 mmol) was dissolved in a minimum volume (ca. 1 mL) of ethyl acetate and the solution was added to a concentrated solution of the respective aminoalcohol **1** in the same solvent (0.10 mmol in ca. 1.5–2.5 mL). The resulting solution was carefully layered with hexane (ca. 8 mL) and the mixture was allowed to crystallise at  $+4^\circ\text{C}$  by diffusion for several days. The dark red, crystalline picrates were isolated by suction, washed with hexane and dried under reduced pressure.

(*Ferrocenylmethyl*)(2-hydroxyethyl)ammonium picrate (**2a**) was obtained from **1a** (26 mg) and picric acid (23 mg). Yield: 45.5 mg (93%). M.p. 163–164  $^\circ\text{C}$  (melting with dec.). Anal. Calc. for  $\text{C}_{19}\text{H}_{20}\text{O}_8\text{N}_4\text{Fe}$  (488.24): C, 46.74; H, 4.13; N, 11.48. Found: C, 46.77; H, 3.99; N, 11.37%.

(*Ferrocenylmethyl*)[2,2-dimethyl-2-hydroxyethyl]ammonium picrate (**2b**) was obtained from **1b** (29 mg) and picric acid (23 mg). Yield: 17 mg (33%). M.p. 159–161  $^\circ\text{C}$  (dec.). Anal. Calc. for  $\text{C}_{21}\text{H}_{24}\text{O}_8\text{N}_4\text{Fe}$  (516.29): C, 48.85; H, 4.69; N, 10.85. Found: C, 48.82; H, 4.64; N, 10.71%.

(*S*)-(Ferrocenylmethyl)[2-(1-methylethyl)-2-hydroxyethyl]ammonium picrate (**2c**) was prepared similarly from **1c** (30 mg) and picric acid (23 mg). Yield: 47.5 mg (90%). M.p. 148–150  $^\circ\text{C}$  (melting), ca. 155  $^\circ\text{C}$  (dec.).  $[\alpha_D]^{23\text{ }^\circ\text{C}} -10^\circ$  ( $c = 1.0$ ,  $\text{MeOH}$ ). Anal. Calc. for  $\text{C}_{22}\text{H}_{26}\text{O}_8\text{N}_4\text{Fe}$  (530.32): C, 49.82; H, 4.94; N, 10.57. Found: C, 50.46; H, 5.14; N, 10.08%.

#### 4.3. X-ray crystallography

Crystals suitable for X-ray diffraction studies were selected directly from the reaction batch (**2a**: red prism,

$0.18 \times 0.28 \times 0.37$  mm<sup>3</sup>; **2c**: red prism,  $0.23 \times 0.23 \times 0.30$  mm<sup>3</sup>; and **2c**: red bar,  $0.10 \times 0.27 \times 0.60$  mm<sup>3</sup>). Full-set diffraction data ( $\pm h \pm k \pm l$ ,  $2\theta \leq 55^\circ$ ) were collected on a Nonius KappaCCD diffractometer equipped with Cryostream Cooler (Oxford Cryosystems). The measurements were performed using graphite-monochromatised Mo  $K\alpha$  radiation ( $\lambda = 0.71073$  Å). Details on the data collection, structure solution and refinement are given in Table 3.

The structures were solved by direct methods (SIR-97 [19]) and refined by full-matrix least-squares routines on  $F^2$  (SHELXL97 [20]). The non-hydrogen atoms were refined with anisotropic displacement parameters. The nitrogen-bonded (H1N and H2N) and hydroxyl (H1O) hydrogens were located on the difference electron density maps and refined as riding atoms with unconstrained isotropic displacement parameters. All other hydrogen atoms were included in the calculated positions and refined as riding atoms.

Final geometric calculations were performed with a recent version of PLATON program [21]. The numerical values were rounded with respect to their estimated standard deviations (ESDs) given with one decimal; parameters involving fixed hydrogen atoms are given without ESDs.

Table 3  
Crystallographic data, structure solution and refinement parameters for **2a–c**<sup>a</sup>

Compound	<b>2a</b>	<b>2b</b>	<b>2c</b>
Formula	$\text{C}_{19}\text{H}_{20}\text{FeN}_4\text{O}_8$	$\text{C}_{21}\text{H}_{24}\text{FeN}_4\text{O}_8$	$\text{C}_{22}\text{H}_{26}\text{FeN}_4\text{O}_8$
$M$ (g mol <sup>-1</sup> )	488.24	516.29	530.32
Crystal system	Triclinic	Monoclinic	Monoclinic
Space group	$P\bar{1}$ (no. 2)	$P2_1/c$ (no. 14)	$P2_1$ (no. 4) <sup>c</sup>
$a$ (Å)	8.1689(2)	12.4417(2)	10.7161(2)
$b$ (Å)	11.4123(3)	14.4118(2)	10.9226(2)
$c$ (Å)	11.4843(3)	13.2273(2)	10.6942(2)
$\alpha$ (°)	98.048(2)		
$\beta$ (°)	103.220(2)	110.842(1)	108.807(1)
$\gamma$ (°)	96.624(2)		
$V$ (Å <sup>3</sup> )	1019.86(5)	2216.55(6)	1184.90(4)
$Z$	2	4	2
$D_{\text{calc}}$ (g mL <sup>-1</sup> )	1.590	1.547	1.486
$\mu$ (Mo $K\alpha$ ) (mm <sup>-1</sup> )	0.796	0.737	0.692
Diffractions collected	15849	41444	20664
Independent/observed <sup>b</sup> diffractions	4662/4275	5067/4152	5393/5036
$R_{\text{int}}^{\text{c}}$ (%)	2.7	4.2	4.0
$R^{\text{c}}$ observed diffractions (%)	2.98	3.49	2.78
$R$ , $wR^{\text{c}}$ all data (%)	3.33, 7.37	4.69, 9.20	3.29, 6.28
$\Delta\rho$ (e Å <sup>-3</sup> )	0.32, -0.52	1.15, <sup>d</sup> -0.44	0.31, -0.26

<sup>a</sup> Common details:  $T = 150(2)$  K.

<sup>b</sup> Diffractions with  $I > 2\sigma(I)$ .

<sup>c</sup> Definitions:  $R_{\text{int}} = \sum |F_o^2 - F_o^2(\text{mean})| / \sum F_o^2$ , where  $F_o^2(\text{mean})$  is the average intensity of symmetry-equivalent diffractions.  $R = \sum ||F_o| - |F_c|| / \sum |F_o|$ ,  $wR = [\sum \{w(F_o^2 - F_c^2)^2\} / \sum w(F_o^2)^2]^{1/2}$ .

<sup>d</sup> Residual electron density in vicinity of the iron atom.

<sup>e</sup> Flack's enantiomorph parameter:  $-0.01(1)$ .

## Acknowledgement

This work is as a part of the long-term research project supported by the Ministry of Education of the Czech Republic (No. MSM0021620857). The authors thank Ing. K. Lang for recording the UV–Vis spectrum of solid **2c** and Ms. A. Jenišová for an assistance during the preparation of **1c**.

## Appendix A. Supplementary material

CCDC 666256, 666257 and 666258 contain the supplementary crystallographic data for this paper. These data can be obtained free of charge from The Cambridge Crystallographic Data Centre via [www.ccdc.cam.ac.uk/data\\_request/cif](http://www.ccdc.cam.ac.uk/data_request/cif). Supplementary data associated with this article can be found, in the online version, at doi:10.1016/j.jorganchem.2008.01.036.

## References

- [1] (a) D. Braga, Chem. Commun. (2003) 2751; (b) D. Braga, F. Grepioni, G.R. Desiraju, Chem. Rev. 98 (1998) 1375; (c) D. Braga, F. Grepioni, Chem. Commun. (1996) 571; , For a general reference, see(d) G.R. Desiraju, Crystal Engineering: Design of Organic Solids, Elsevier, Amsterdam, 1989.
- [2] (a) A. Togni, T. Hayashi (Eds.), Ferrocenes: Homogeneous Catalysis, Organic Synthesis, Material Science, VCH, Weinheim, 1995; (b) S. Barlow, S.R. Marder, Chem. Commun. (2000) 1555; (c) N.J. Long, Angew. Chem., Int. Ed. Engl. 34 (1995) 21.
- [3] (a) C.M. Zakaria, G. Ferguson, A.J. Lough, C. Glidewell, Acta Crystallogr., Sect. C, Cryst. Struct. Commun. 57 (2001) 687; (b) D. Braga, L. Maini, F. Paganelli, E. Tagliavini, S. Casolari, F. Grepioni, J. Organomet. Chem. 637–639 (2001) 609; (c) C.M. Zakaria, G. Ferguson, A.J. Lough, C. Glidewell, Acta Crystallogr., Sect. B, Struct. Sci. 58 (2002) 786; (d) C.M. Zakaria, G. Ferguson, A.J. Lough, C. Glidewell, Acta Crystallogr., Sect. C, Cryst. Struct. Commun. 59 (2003) 271; (e) D. Braga, L. Maini, M. Polito, L. Mirolo, F. Grepioni, Chem. Eur. J. 9 (2003) 4362.
- [4] (a) G. Ferguson, J.F. Gallagher, C. Glidewell, C.M. Zakaria, Acta Crystallogr., Sect. C 19 (1993) 967; (b) J.F. Gallagher, G. Ferguson, C. Glidewell, C.M. Zakaria, Acta Crystallogr., Sect. C 50 (1994) 18; (c) C. Glidewell, G. Ferguson, A.J. Lough, C.M. Zakaria, J. Chem. Soc., Dalton Trans. (1994) 1971; (d) C. Glidewell, C.M. Zakaria, G. Ferguson, C. Glidewell, C.M. Zakaria, Acta Crystallogr., Sect. C 50 (1994) 678; (e) G. Ferguson, C. Glidewell, A. Lewis, C.M. Zakaria, J. Organomet. Chem. 492 (1995) 229; (f) C. Glidewell, R.B. Klar, P. Lightfoot, C.M. Zakaria, G. Ferguson, Acta Crystallogr., Sect. B 52 (1996) 110; (g) W. Bell, G. Ferguson, C. Glidewell, Acta Crystallogr., Sect. C 52 (1996) 3009; (h) C. Glidewell, S.Z. Ahmed, J.F. Gallagher, G. Ferguson, Acta Crystallogr., Sect. C 53 (1997) 1775; (i) C.M. Zakaria, G. Ferguson, A.J. Lough, C. Glidewell, Acta Crystallogr., Sect. C, Cryst. Struct. Commun. 57 (2001) 914; (j) C.M. Zakaria, G. Ferguson, A.J. Lough, C. Glidewell, Acta Crystallogr., Sect. C, Cryst. Struct. Commun. 58 (2002) m1; (k) C.M. Zakaria, G. Ferguson, A.J. Lough, C. Glidewell, Acta Crystallogr., Sect. C, Cryst. Struct. Commun. 58 (2002) m5.
- [5] (a) D.M. Shin, Y.K. Chung, I.S. Lee, Cryst. Growth Des. 2 (2002) 493; (b) I.S. Lee, D.M. Shin, Y.K. Chung, Cryst. Growth Des. 3 (2003) 521; (c) D. Braga, M. Polito, M. Braccacini, D. D'Addario, E. Tagliavini, L. Sturba, Organometallics 22 (2003) 2142; (d) D. Braga, M. Polito, D. D'Addario, E. Tagliavini, D.M. Proserpio, F. Grepioni, J.W. Steed, Organometallics 22 (2003) 4532; (e) R. Horikoshi, C. Nambu, T. Mochida, New J. Chem. 28 (2004) 26; (f) T. Mochida, K. Okazawa, R. Horikoshi, Dalton Trans. (2006) 693; (g) Y. Gao, B. Twamley, J.M. Shreeve, Organometallics 25 (2006) 3364; (h) T. Mochida, F. Shimizu, H. Shimizu, K. Okazawa, F. Sato, D. Kuwahara, J. Organomet. Chem. 692 (2007) 1834.
- [6] A.D. Burrows, Struct. Bond. 108 (2004) 55.
- [7] (a) G.R. Desiraju, Chem. Commun. (2005) 2995; (b) G.R. Desiraju, Acc. Chem. Res. 35 (2002) 565; (c) T. Steiner, Angew. Chem., Int. Ed. 41 (2002) 48; (d) G.R. Desiraju, J. Chem. Soc., Dalton Trans. (2000) 3745; (e) G.A. Jeffrey, An Introduction to Hydrogen Bonding, Oxford University Press, New York, 1997; (f) G.R. Desiraju, Angew. Chem., Int. Ed. Engl. 34 (1995) 2311; (g) C.A. Hunter, K.R. Lawson, J. Perkins, C.J. Urch, J. Chem. Soc., Perkin Trans. 2 (2001) 651, and references therein; (h) L.R. Hanton, C.A. Hunter, D.H. Purvis, J. Chem. Soc., Chem. Commun. (1992) 1134.
- [8] P. Štěpnička, I. Císařová, New J. Chem. 26 (2002) 1389.
- [9] P. Štěpnička, I. Císařová, CrystEngComm 7 (2005) 37.
- [10] P. Štěpnička, I. Císařová, J. Ludvík, J. Organomet. Chem. 689 (2004) 631.
- [11] (a) A. Hess, O. Brosch, T. Weyhermueller, N. Metzler-Nolte, J. Organomet. Chem. 589 (1999) 75; See also: (b) J.L. Kerr, J.S. Landells, D.S. Larsen, B.H. Robinson, J. Simpson, J. Chem. Soc., Dalton Trans. (2000) 1411.
- [12] UV–Vis spectrum of **1c** recorded in a methanol solution shows two bands at 322 and 436 nm but the associated molar absorption coefficients are about two orders of magnitude lower than those for picric acid.
- [13] (a) M.L.H. Green, S.R. Marder, M.E. Thompson, J.A. Bandy, J. Bloor, P.V. Kolinsky, R.J. Jones, Nature 330 (1987) 360; (b) E. Peris, Coord. Chem. Rev. 248 (2004) 279; (c) B. Bildstein, Coord. Chem. Rev. 206–207 (2000) 369; (d) T. Verbiest, S. Houbrechts, M. Kauranen, K. Clays, A. Persoons, J. Mater. Chem. 7 (1997) 2175; (e) S.K. Pal, A. Krishan, P.K. Das, A.G. Samuelson, J. Organomet. Chem. 637–639 (2001) 827; (f) D.M. Shin, I.S. Lee, Y.K. Chung, Eur. J. Inorg. Chem. (2003) 2311.
- [14] (a) P. Srinivasan, M. Gunasekaran, T. Kanagasekaran, R. Gopalakrishnan, P. Ramasamy, J. Cryst. Growth 289 (2006) 639, and references therein; (b) P. Srinivasan, M. Gunasekaran, T. Kanagasekaran, R. Gopalakrishnan, G. Bhagavannarayana, P. Ramasamy, Cryst. Growth Des. 6 (2006) 1663; (c) K. Kondo, N. Ohnishi, K. Takemoto, H. Yoshida, K. Yoshiga, J. Org. Chem. 57 (1992) 1622.
- [15] N.S. Poonia, R. Chandra, W.S. Sheldrick, Bull. Chem. Soc. Jpn. 63 (1990) 1512.
- [16] K. Frydenwang, B. Jensen, K. Nielsen, Acta Crystallogr., Sect. C 48 (1992) 1343.
- [17] V.N. Solovyev, A.N. Chekhlov, R.G. Gafurov, V.G. Chistyakov, I.B. Martynov, Zh. Strukt. Khim. 29 (1988) 174.
- [18] S.K. Kurtz, T.T. Perry, J. Appl. Phys. 39 (1968) 3798.
- [19] A. Altomare, M.C. Burla, M. Camalli, G.L. Casciaro, C. Giacovazzo, A. Guagliardi, A.G.G. Moliterni, G. Polidori, R. Spagna, J. Appl. Crystallogr. 32 (1999) 115.
- [20] G.M. Sheldrick, SHELXL97 Program for Crystal Structure Refinement from Diffraction Data, University of Goettingen, Germany, 1997.
- [21] A.L. Spek, Platon, A Multipurpose Crystallographic Tool, Utrecht University, Utrecht, The Netherlands, 2007. Distributed via Internet at <http://www.cryst.chem.uu.nl/platon/>.